Available online at BCREC website: https://bcrec.id

Bulletin of Chemical Reaction Engineering & Catalysis, 16 (2) 2021, 310-319

Research Article

Activity Enhancement of P25 Titanium Dioxide by Zinc Oxide for Photocatalytic Phenol Degradation

Yehezkiel Steven Kurniawan[1], Leny Yuliati[1,2,*)]

[1]Ma Chung Research Center for Photosynthetic Pigments, Universitas Ma Chung, Malang 65151, East Java, Indonesia.
[2]Department of Chemistry, Faculty of Science and Technology, Universitas Ma Chung, Malang 65151, East Java, Indonesia.

Received: 8th February 2021; Revised: 8th April 2021; Accepted: 9th April 2021
Available online: 12nd April 2021; Published regularly: June 2021

Abstract

As a benchmark photocatalyst, P25 titanium dioxide (TiO_2) nanomaterial has been widely reported for its remarkable photocatalytic activity under ultraviolet (UV) irradiation. However, approaches to further improve the photocatalytic activity of the P25 TiO_2 are still required. In the present work, we reported the activity enhancement of the P25 TiO_2 up to more than five times higher rate constant for phenol degradation when the P25 TiO_2 was coupled with zinc oxide (ZnO). The composites were prepared by a physical mixing method of P25 TiO_2 and ZnO with various weight ratios of 1:0.5, 1:1, and 1:2. The composite materials were then characterized using X-ray diffraction (XRD), diffuse-reflectance ultraviolet-visible (DR UV-vis), Fourier transform infrared (FTIR), and fluorescence spectroscopies. All the composites gave better activity than the P25 TiO_2, in which the TiO_2/ZnO 1:1 composite material exhibited the highest first-order reaction rate constant (0.43 h^{-1}). This remarkable enhanced degradation rate was much higher than that of the unmodified TiO_2 (0.08 h^{-1}) and ZnO (0.13 h^{-1}). The fluorescence study revealed that the electron-hole recombination on the P25 TiO_2 could be suppressed by the ZnO, which would be the reason for such activity enhancement. A study on the effect of the scavenger showed that the hydroxyl radicals played a crucial role in the photocatalytic phenol degradation.

Keywords: Electron-hole recombination; P25 TiO_2; Phenol degradation; Photocatalyst; ZnO

How to Cite: Y.S. Kurniawan, L. Yuliati (2021). Activity Enhancement of P25 Titanium Dioxide by Zinc Oxide for Photocatalytic Phenol Degradation. *Bulletin of Chemical Reaction Engineering & Catalysis*, 16(2), 310-319 (doi:10.9767/bcrec.16.2.10319.310-319)

Permalink/DOI: https://doi.org/10.9767/bcrec.16.2.10319.310-319

1. Introduction

Phenolic compounds have polluted our aquatic environment and caused serious health damages such as irritation, nausea, diarrhea, hemolytic anemia, and pulmonary edema [1]. Many efforts have been developed in wastewater remediation to eliminate or at least reduce the phenol concentration through several techniques, such as: adsorption [2], photocatalysis [3,4], and bioremediation [5]. Adsorption is the simplest technique to reduce the phenol concentration, however, the used adsorbent material needs to be further processed for a recycling process [2]. On the other hand, the photocatalysis method offers the total elimination of phenol to less toxic compounds of carbon dioxide (CO_2) and water (H_2O), but with a relatively slow degradation rate. Combining the adsorption and photocatalysis techniques would be a great op-

* Corresponding Author.
Email: leny.yuliati@machung.ac.id (L. Yuliati);
Telp: +62-341-550171, Fax: +62-341-550175

tion to reduce the wastewater problems. When metal oxide semiconductor materials are used as the adsorbent material, the further process could be easily carried out by irradiating the mixture under ultraviolet (UV) light as named as a photocatalytic process [6–10]. This photocatalytic process is one of the environmental-friendly processes because the end products are CO_2 and H_2O, and the catalyst materials can be easily regenerated after the photocatalysis process.

Among several metal oxides, the P25 titanium dioxide (TiO_2) nanomaterial has been known for its remarkable degradation activity under UV irradiation [11–15]. Nevertheless, the charge recombination on the photocatalyst limits its photocatalytic efficiency and thus, a complete photodegradation process takes a long time. The addition of other metal oxides, such as: copper oxides [11,12] and cobalt oxides [13], was reported, but the improved activity was quite low. Other approaches are adding the dye sensitizer [16], coupling the TiO_2 with another semiconductor [17–19] such as zinc oxide (ZnO) semiconductor that may prevent electron-hole recombination and enhance photocatalytic activity [17]. Whilst the TiO_2/ZnO composite material can be prepared through sol-gel [17,18], solid-state sintering [20], and the physical mixing [21,22] methods, the physical mixing technique is the simplest one to prepare TiO_2/ZnO composite materials. It was reported that the ZnO and TiO_2 were physically mixed to obtain TiO_2/ZnO composite materials for cosmetic [21] and dye-sensitized solar cell [22] purposes. As for photocatalytic applications, several composites have been prepared by the physical mixing method, such as: TiO_2-carbon nitride [19], ZnO-carbon nitride [23], and ZnO-graphene-TiO_2 [24]. Since the physical mixing method does not involve any heat treatments, this method would maintain the original properties of the P25 TiO_2 and ZnO. To the best of our knowledge, the activity performance of P25 TiO_2 after physically mixed with commercial ZnO has not been evaluated yet.

In this work, we demonstrated that the large enhancement of photocatalytic activity in the P25 TiO_2 could be achieved when the composite was prepared by a simple physical mixing method. We prepared three types of TiO_2/ZnO composite materials with different weight ratios, *i.e.* TiO_2/ZnO 1:0.5, TiO_2/ZnO 1:1, and TiO_2/ZnO 1:2. The composite materials were characterized using diffuse-reflectance ultraviolet-visible (DR UV-vis), Fourier transform infrared (FTIR), and fluorescence spectroscopies. Their adsorption capability for phenol at a dark condition was conducted, and then their photocatalytic activity towards phenol degradation was evaluated. By varying the irradiation time, the kinetic model for phenol photodegradation was also discussed. Besides, the active species for photodegradation of phenol was proposed based on the scavenging experiments.

2. Materials and Methods

2.1 Materials

Phenol (C_6H_5OH, 99%), silver nitrate ($AgNO_3$, 99.9%), diammonium oxalate monohydrate ($(NH_4)_2C_2O_4 \cdot H_2O$, 99.5%), and *tert*-butanol (^tBuOH, $(H_3C)_3COH$, 99%) were obtained from Merck in pro analysis grade. Acetonitrile (CH_3CN, $\geq$99.9%) that was used as the mobile phase during analysis was also obtained from Merck. The commercial ZnO and P25 TiO_2 were received from Fagron Chemicals and Evonik Industries, respectively. Based on the certificate of analysis, the specific surface area of ZnO was stated to be 4.5 $m^2.g^{-1}$ as the lower limit. These chemicals were used without any further purifications.

2.2 Preparation of TiO_2/ZnO Composite Materials

The TiO_2/ZnO composite materials were prepared by physical mixing of commercial P25 TiO_2 and ZnO to obtain TiO_2/ZnO 1:0.5, TiO_2/ZnO 1:1, and TiO_2/ZnO 1:2. The TiO_2/ZnO 1:0.5 material was prepared by mixing 1.0 g of P25 TiO_2 and 0.5 g of ZnO, the TiO_2/ZnO 1:1 material was prepared by mixing 1.0 g of P25 TiO_2 and 1.0 g of ZnO, while the TiO_2/ZnO 1:2 material was prepared by mixing 1.0 g of P25 TiO_2 and 2.0 g of ZnO. The mixture was carefully ground with the help of a mortar.

2.3 Characterizations of TiO_2/ZnO Composite Materials

The prepared TiO_2/ZnO composite materials were characterized using XRD, DR UV-vis, FTIR, and spectrofluorometer. The diffraction patterns of P25 TiO_2, ZnO, and the TiO_2/ZnO 1:1 composite were recorded at room temperature on an X-ray diffractometer (PANalytical X'Pert^3 Powder). The DR UV-vis spectrum was recorded using a UV-vis spectrophotometer (JASCO V-760) from 200–800 nm to identify the absorption signal of the composite material. Furthermore, the bandgap energy of the composite material was determined using the Tauc plot as shown in Equation (1).

$$(\alpha h\upsilon) = A(Eg - h\upsilon) \quad (1)$$

whereas α, h, υ, and Eg are the absorption coefficient of the materials, Planck constant, light frequency, and bandgap energy, respectively. The Kubelka-Munk function has been generally used to replace the α value [25], which was also adopted in this work.

The FTIR spectrum of the composite material was recorded through the ATR method using an FTIR spectrophotometer (JASCO FTIR-6800) for 400–4000 cm^{-1} measurement range. The excitation and emission spectra of the TiO_2/ZnO composite material were recorded on a solid sample holder using a spectrofluorometer (JASCO FP-8500).

2.4 Adsorption of Phenol using TiO_2/ZnO Composite Materials

As photocatalytic degradation of phenol would only occur after the adsorption process, the equilibrium of phenol adsorption in dark condition was investigated. The photocatalyst material (50 mg) was added into 50 $mg.L^{-1}$ of aqueous phenol solution (50 mL) and stirred for 60 minutes. The phenol concentration was measured using a high-performance liquid chromatography (HPLC, Shimadzu LC-20 AT) with a photodiode array detector (PDA, SPD-M20A). The used stationary phase was the C18 column at 40 °C as the set temperature, while the mobile phase was 100% acetonitrile at 0.8 $mL.min^{-1}$ flow rate. The phenol adsorption percentage was then calculated using Equation (2), where the $[PhOH]_0$ represented the initial phenol concentration and the $[PhOH]_a$ showed the phenol concentration after adsorption for 60 minutes.

$$Adsorption(\%) = \frac{[PhOH]_0 - [PhOH]_a}{[PhOH]_0} x100\% \quad (2)$$

2.5 Photodegradation of Phenol using TiO_2/ZnO Composite Materials

The photocatalyst (50 mg) was added into the aqueous solution of phenol (50 $mg.L^{-1}$, 50 mL) and stirred for 60 minutes in dark condition. After the adsorption process, the mixture was irradiated using an ultraviolet lamp (UVLS-28 EL Series, 365 nm) for 1, 2, 3, 4, and 5 h. Afterward, the phenol concentration was measured, and the phenol degradation percentage was calculated using Equation (3). The $[PhOH]_t$ represented the phenol concentration after each reaction. The kinetic analysis was carried out using zeroth-, first-, and second-order kinetic models.

$$Photodegradation\ (\%) = \frac{[PhOH]_a - [PhOH]_t}{[PhOH]_a} x100\% \quad (3)$$

2.6 Effect of the Scavenger Agent on the Phenol Photodegradation

The TiO_2/ZnO 1:1 photocatalyst material (50 mg) as the representative composite material was added into the aqueous solution of phenol (50 $mg.L^{-1}$, 50 mL) and stirred for 60 minutes at dark condition. After the adsorption process, the mixture was added by scavenger agent ($AgNO_3$ (45.12 mg, 0.26 mmol, 10 equiv.) or $(NH_4)_2C_2O_4 \cdot H_2O$ (37.74 mg, 0.26 mmol, 10 equiv.) or ^tBuOH (19.69 mg, 0.26 mmol, 10 equiv.)), and then the mixture was irradiated using the UV lamp for 2 h. Afterward, the phenol concentration was measured and the phenol photodegradation percentage was calculated using Equation 3.

3. Results and Discussions

3.1 Characterizations of TiO_2/ZnO Composite Materials

The crystal structure of P25 TiO_2, ZnO, and TiO_2/ZnO 1:1 as the representative of the composite materials were identified from the XRD measurement. The diffractograms of P25 TiO_2, ZnO, and TiO_2/ZnO 1:1 material are shown in Figure 1. The P25 TiO_2 have both anatase and rutile phases, in good agreement with other reported literature [11–14], while the ZnO composed of wurtzite crystal phase [26]. Since the TiO_2/ZnO composite materials were prepared through a simple physical mixing technique, the TiO_2/ZnO 1:1 composite material consisted of anatase and rutile TiO_2 as well as ZnO wurtzite crystal phases. This result clarified that the crystal structure of either TiO_2

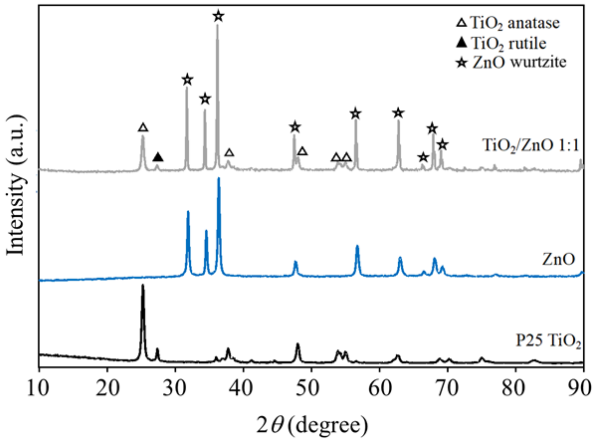

Figure 1. XRD patterns of TiO_2, ZnO, and TiO_2/ZnO 1:1 materials.

(anatase and rutile) or ZnO (wurtzite) framework was not significantly changed on the TiO_2/ZnO composite.

The optical properties of the composites were further examined. As depicted in Figure 2, all the composites of TiO_2/ZnO 1:0.5, TiO_2/ZnO 1:1, and TiO_2/ZnO 1:2 materials were obtained as white powders, which were similar to the color of P25 TiO_2 and ZnO. The DR UV-vis spectra of the unmodified TiO_2, ZnO, and the composites are shown in Figure 3. As expected, the TiO_2, ZnO, and the composites only showed strong absorption in UV region and no absorption was observed above 400 nm due to their white color. The composites exhibited absorption edge between the absorption edge of TiO_2 and ZnO, indicating the presence of both TiO_2 and ZnO in the composites. The bandgap energy was then calculated by the Tauc plot. The bandgap energy values of TiO_2/ZnO 1:2, TiO_2/ZnO 1:1, and TiO_2/ZnO 1:0.5 composites were determined to be 3.22, 3.20, and 3.20 eV, respectively. These values were between the bandgap energy values of TiO_2 (3.32 eV) and ZnO (3.19 eV). It was clear that when the amount of ZnO was higher, the optical character of the composites was more resembled to the ZnO.

The FTIR spectra of TiO_2, ZnO, and TiO_2/ZnO composite materials are shown in Figure 4. The TiO_2 has the vibration peak of −OH groups, which could be observed around 3,350 cm^{-1}, and the vibration of Ti−O−Ti that could be seen at 657 cm^{-1} [27]. The TiO_2 and ZnO showed the vibration of M−O linkages (Ti−O or Zn−O) that could be clarified from the vibration peak at 438 cm^{-1} [28]. All composites showed the vibration peaks that were also detected in the TiO_2 and ZnO, indicating that the composites have both the TiO_2 and ZnO. When the ratio amount of ZnO increased, both signals of the hydroxyl groups at 3,350 cm^{-1} and the Ti−O−Ti linkages at 657 cm^{-1} decreased, giving similar absorption peaks as those observed on the ZnO.

The fluorescence spectra of TiO_2, ZnO, and TiO_2/ZnO composite materials are shown in Figure 5. Since the composites have both characters of TiO_2 and ZnO, the fluorescence spectra were measured from the point of view of excitation and emission of both TiO_2 and ZnO. As shown in Figures 5(a) and (b), TiO_2 showed excitation peak at 216 nm when monitored at emission wavelength of 274 nm, and emission peaks at 274, 405, and 540 nm when monitored at excitation wavelength of 216 nm. The intensity of excitation and emission peaks of TiO_2 decreased with the addition of ZnO. It was noted that among the composites, the TiO_2/ZnO 1:1 gave the lowest intensity. Since the lower

Figure 2. Photographs of TiO_2, ZnO and TiO_2/ZnO composites.

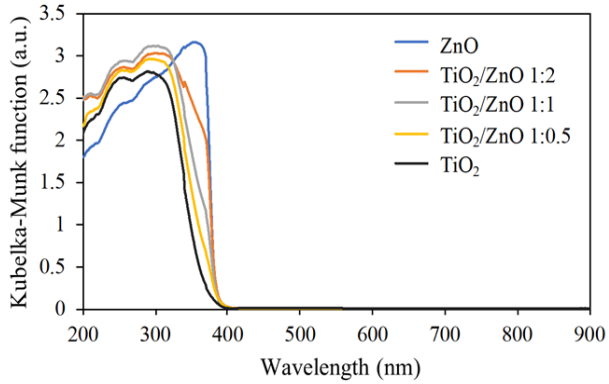

Figure 3. DR UV-vis spectra of TiO_2, ZnO, and TiO_2/ZnO composites.

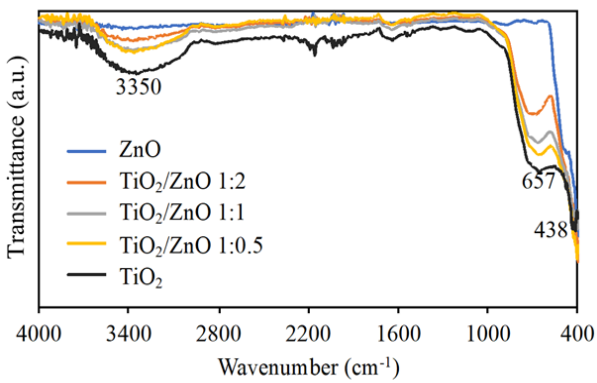

Figure 4. FTIR spectra of TiO_2, ZnO, and TiO_2/ZnO composites.

emission intensity has been correlated to the lower electron-hole recombination, the addition of ZnO was shown to result in the lower electron-hole recombination on the TiO_2. Figures 5(c) and (d) showed the excitation and emission spectra of ZnO and composite materials. ZnO gave excitation and emission peaks at 378 nm and 516 nm, respectively. The TiO_2/ZnO composites gave similar excitation peak to that of ZnO. However, when the amount of ZnO was low, an additional excitation peak at 279 nm could be observed in the TiO_2/ZnO 1:1 and TiO_2/ZnO 1:0.5 composites, which could come from the TiO_2. Furthermore, the excitation and emission intensity of ZnO tended to increase with the addition of TiO_2. This result showed that the electron-hole recombination on the ZnO was not suppressed by the addition of TiO_2. In other words, the charge transfer shall occur from TiO_2 to ZnO, but not vice versa.

3.2 Adsorption and Photodegradation of Phenol

The adsorption of phenol was carried out in dark condition to evaluate the adsorption capability of TiO_2/ZnO composite materials in comparison to P25 TiO_2 and ZnO materials. The adsorption percentages of phenol using the P25 TiO_2, ZnO, and TiO_2/ZnO composite materials are shown in Figure 6. The TiO_2/ZnO composites gave the phenol adsorption percentages (8.31–8.51%) in between P25 TiO_2 (1.36%) and ZnO (10.64%) materials. As indicated in the literature [14], the specific surface area of P25 TiO_2 was *ca.* 50 $m^2.g^{-1}$, which value was more than ten times higher than that of the ZnO (*ca.* 4.5 m^2 g^{-1}). While the high adsorption could be related to the large specific surface area, this

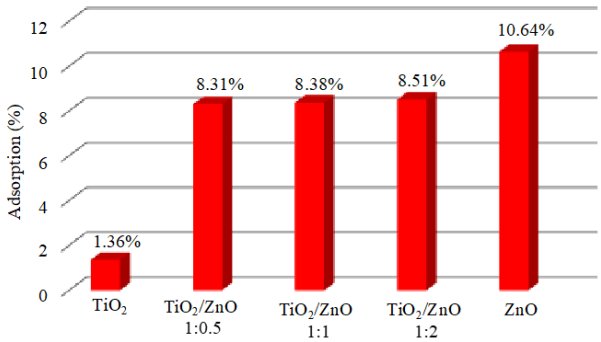

Figure 6. Phenol adsorption on TiO_2, ZnO, and TiO_2/ZnO composites.

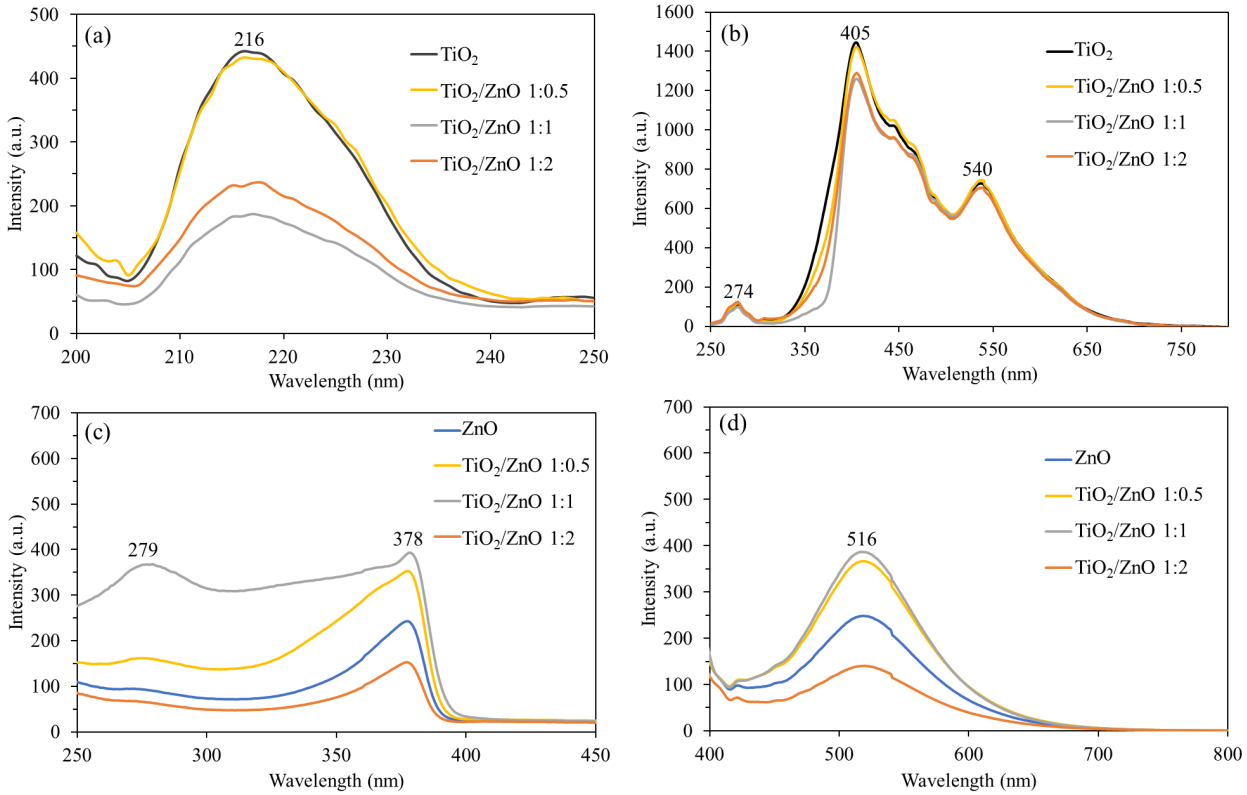

Figure 5. Excitation (a) and emission spectra (b) of TiO_2 and composite materials monitored at emission and excitation wavelengths of 274 and 216 nm, respectively, excitation (c) and emission (d) of ZnO and composite materials monitored at emission and excitation wavelengths of 516 and 378 nm, respectively.

result showed that it is not always the case as the ZnO could adsorb better than the TiO_2 P25. Further study is still required to explain this phenomenon.

From the photocatalytic reaction results, it was found that the TiO_2/ZnO composite materials gave higher photocatalytic degradation percentages of phenol than either P25 TiO_2 or ZnO materials, which is remarkable. As shown in Figure 7, after 5 h-reaction, the P25 TiO_2 and ZnO only gave phenol degradation of 30.65% and 47.82%, respectively, while the TiO_2/ZnO 1:0.5, TiO_2/ZnO 1:1, and TiO_2/ZnO 1:2 materials exhibited 94.03%, 99.51% and 73.00%, respectively. Among the composites, the TiO_2/ZnO 1:1 gave the best photocatalytic activity for phenol degradation.

The kinetic of photocatalytic phenol degradation was evaluated using zeroth-, first-, and second-order model. The kinetic results are listed in Table 1. It was confirmed that the photocatalytic phenol degradation followed the first-order model as it has the highest correlation factor (R^2) among other kinetic models. The order of the reaction rate constant is TiO_2/ZnO 1:1 > TiO_2/ZnO 1:0.5 > TiO_2/ZnO 1:2 > ZnO > TiO_2, as shown in Table 2. All of the TiO_2/ZnO composite materials exhibited re-

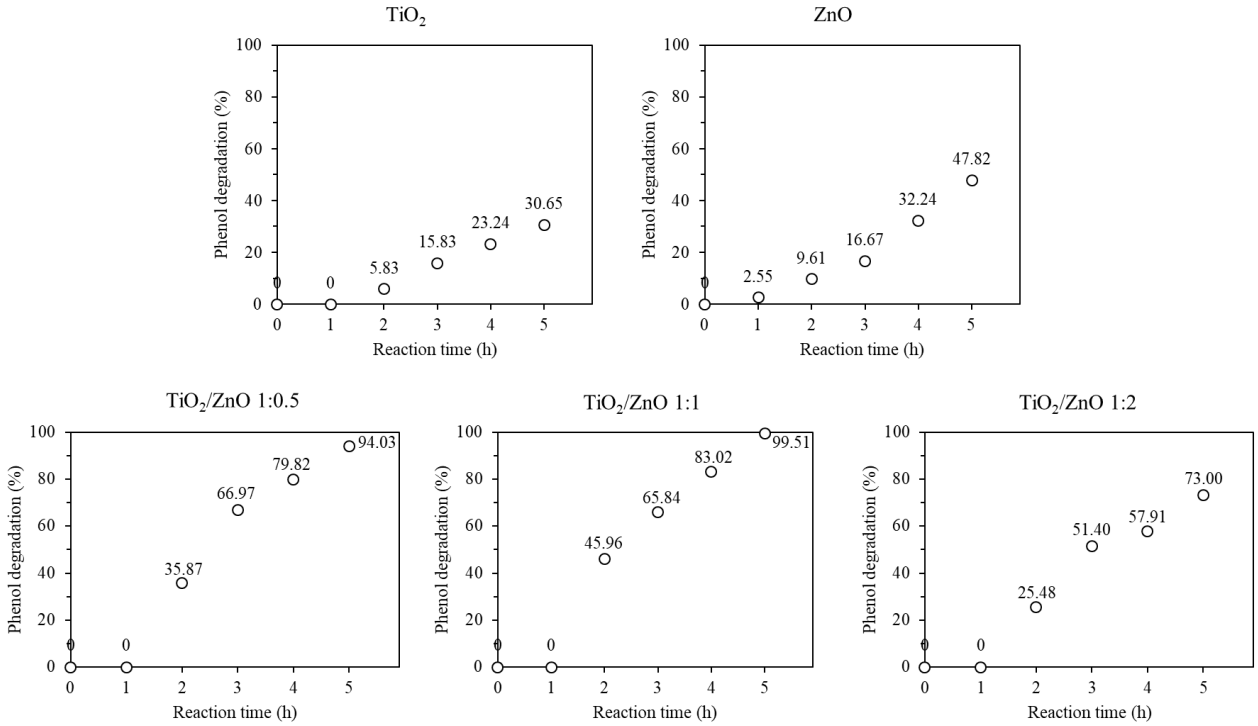

Figure 7. Time profiles of phenol degradation on TiO_2, ZnO, and TiO_2/ZnO composites.

Table 1. Kinetic models of phenol photodegradation on TiO_2, ZnO, and TiO_2/ZnO composite materials.

	Zeroth-order $[PhOH]_t = -kt + [PhOH]_0$	First-order $\ln([PhOH]_t) = -kt + \ln([PhOH]_0)$	Second order $[PhOH]_t^{-1} = kt + [PhOH]_0^{-1}$
TiO_2	$[PhOH]_t = -3.23t + 50.5$ $R^2 = 0.9538$	$\ln([PhOH]_t) = -0.08t + 3.93$ $R^2 = 0.9451$	$[PhOH]_t^{-1} = 0.002t + 0.019$ $R^2 = 0.9322$
ZnO	$[PhOH]_t = -4.13t + 45.7$ $R^2 = 0.9297$	$\ln([PhOH]_t) = -0.13t + 3.86$ $R^2 = 0.8862$	$[PhOH]_t^{-1} = 0.004t - 0.020$ $R^2 = 0.8331$
TiO_2/ZnO 1:0.5	$[PhOH]_t = -9.28t + 45.3$ $R^2 = 0.9435$	$\ln([PhOH]_t) = -0.40t + 3.92$ $R^2 = 0.9843$	$[PhOH]_t^{-1} = 0.021t + 0.011$ $R^2 = 0.8410$
TiO_2/ZnO 1:1	$[PhOH]_t = -9.58t + 45.0$ $R^2 = 0.9596$	$\ln([PhOH]_t) = -0.43t + 3.92$ $R^2 = 0.9958$	$[PhOH]_t^{-1} = 0.024t + 0.009$ $R^2 = 0.8025$
TiO_2/ZnO 1:2	$[PhOH]_t = -6.86t + 45.2$ $R^2 = 0.9523$	$\ln([PhOH]_t) = -0.23t + 3.85$ $R^2 = 0.9690$	$[PhOH]_t^{-1} = 0.008t + 0.020$ $R^2 = 0.9223$

markable higher reaction rate constants than the TiO_2 and ZnO, demonstrating that the composites are better photocatalysts than the unmodified ones. More than five times faster degradation rate than the P25 TiO_2 could be observed on the TiO_2/ZnO 1:1 composite.

The higher photocatalytic activity of those composite materials than the unmodified TiO_2 and ZnO could be a sign that the electron-hole recombination was successfully reduced. From the fluorescence spectra discussed in Figure 5, it was proposed that the electron transfer in the TiO_2/ZnO would occur from TiO_2 to ZnO. In order to elucidate the active species responsible for the photocatalytic phenol degradation, we investigated the effect of the scavenger agent on the activity using TiO_2/ZnO 1:1 as the representative of the composite materials. The $AgNO_3$, $(NH_4)_2C_2O_4$, and ^{t}BuOH were used as the scavenging agent for electron (e^-), hole (h^+), and hydroxyl radical (HO•), respectively [29–31].

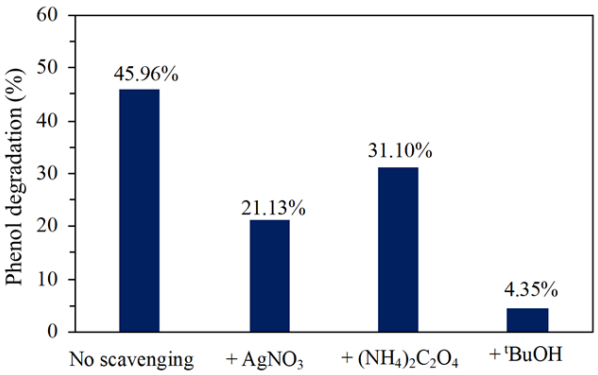

Figure 8. Effect of scavenger agents in the phenol photodegradation process on TiO_2/ZnO 1:1 composite.

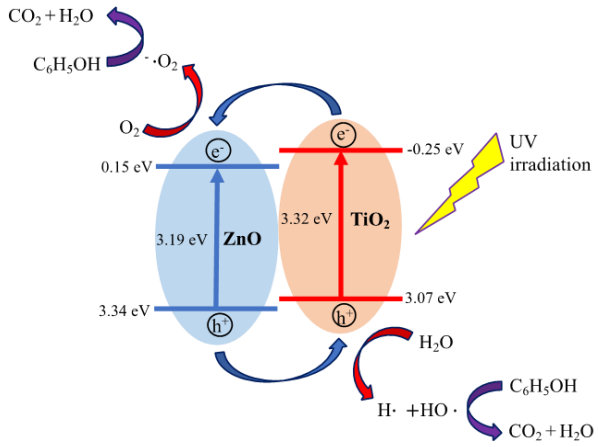

Figure 9. Proposed mechanism of phenol photodegradation on TiO_2/ZnO composite materials.

The effect of the scavenger agent on the phenol photodegradation process using TiO_2/ZnO 1:1 is shown in Figure 8. It was found that after the addition of $AgNO_3$, $(NH4)_2C_2O_4$, and ^{t}BuOH, the phenol photodegradation percentage was quenched from 45.96% to 21.13%, 31.10%, and 4.35%, respectively. This result showed that electrons, holes, and hydroxyl radicals affected the phenol photodegradation, but since the decrement of phenol photodegradation percentage for hydroxy radical scavenging was the highest one, hydroxyl radicals would play as the main active species in the degradation process.

Figure 9 shows the proposed photodegradation mechanism of phenol using TiO_2/ZnO composite materials. The valence band of ZnO and TiO_2 were adopted from the previous reports [32,33]. Since the phenol oxidation potential (2.10 eV) is located between the valence band and conduction band of the composite materials, the phenol oxidation spontaneously occurs [34]. At first, under UV light irradiation the electrons at the valence bands of TiO_2 and ZnO would be excited. The excited electrons would be transferred from the conduction band of TiO_2 to the conduction band of ZnO and consequently, the holes would be transferred from the valence band of ZnO to the valence band of TiO_2. This would reduce the electron-hole recombination on the TiO_2. Therefore, the reduction of oxygen would mainly happen on the conduction band of ZnO while the oxidation of water would mainly happen on the valence band of TiO_2. The generated hydroxyl radicals would play as the main species for photocatalytic degradation of phenol. Since hydroxyl and oxygen radicals are available due to the prevention of the charge recombination, phenol can be completely degraded to form CO_2 and H_2O.

Table 2. The first-order rate constants of phenol photodegradation on TiO_2, ZnO, and TiO_2/ZnO composite materials.

Photocatalyst materials	k (h^{-1})
TiO_2	0.08
ZnO	0.13
TiO_2/ZnO 1:0.5	0.40
TiO_2/ZnO 1:1	0.43
TiO_2/ZnO 1:2	0.23

4. Conclusions

Three types of TiO_2/ZnO composite materials, *i.e.* TiO_2/ZnO 1:0.5, TiO_2/ZnO 1:1, and TiO_2/ZnO 1:2, were obtained as white powders through physical mixing technique of P25 TiO_2 and ZnO. XRD patterns confirmed that the TiO_2/ZnO 1:1 composite has the crystal phases of anatase and rutile TiO_2 as well as wurtzite ZnO, originating from the P25 TiO_2 and ZnO. DR UV-Vis spectra revealed that the absorption edge and band gap energy values of the composites were between those of the TiO_2 and ZnO. FTIR spectra showed that the composites have the characters of both TiO_2 and ZnO. The fluorescence study clarified the reduction of electron-hole recombination on the TiO_2 with the addition of ZnO. Adsorption test showed that the composites gave better results than the TiO_2, but lower than that of the ZnO. All the TiO_2/ZnO composites gave better photocatalytic activity than the TiO_2 and ZnO. The best composite, the TiO_2/ZnO 1:1, exhibited the highest phenol photodegradation (99.51%) after 5 h-reaction, which was much higher than P25 TiO_2 (30.65%) and ZnO (47.82%). The phenol degradation was shown to follow the first order kinetic model. More than five times faster degradation rate was observed as compared to the P25 TiO_2 as a result of the inhibited electron-hole recombination. Scavenger study confirmed that hydroxyl radicals were the main species that played a pivotal role in the phenol photodegradation process.

Acknowledgment

The financial support from the Directorate General of Strengthening Research and Development, Ministry of Research and Technology/National Research and Innovation Agency of Indonesia through the Higher Education Excellent Applied Research Grant (PTUPT 2020, No. 041/SP2H/AMD/LT/MULTI/L7/2020 and No. 002/MACHUNG/LPPM/SP2H-LIT-MULTI/AMD/VI/2020) is greatly acknowledged.

References

[1] Babich, H., Davis, D.L. (1981). Phenol: A review of environmental and health risks. *Regulatory Toxicology and Pharmacology*, 1, 90–109. DOI: 10.1016/0273-2300(81)90071-4.

[2] Issabayeva, G., Hang, S.Y., Wong, M.C., Aroua, M.K. (2018). A review on the adsorption of phenols from wastewater onto diverse groups of adsorbents. *Reviews in Chemical Engineering,* 34, 855–873. DOI: 10.1515/revce-2017-0007.

[3] Ahmed, S., Rasul, M.G., Martens, W.N., Brown, R., Hashib, M.A. (2010). Heterogeneous photocatalytic degradation of phenols in wastewater: A review on current status and developments. *Desalination*, 261, 3–18. DOI: 10.1016/j.desal.2010.04.062.

[4] Ahmed, S., Rasul, M.G., Martens, W.N., Brown, R., Hashib, M.A. (2010). Advances in heterogeneous photocatalytic degradation of phenols and dyes in wastewater: A review. *Water, Air, & Soil Pollution,* 215, 3–29. DOI: 10.1007/s11270-010-0456-3.

[5] Poi, G., Aburto-Medina, A., Mok, P.C., Ball, A.S., Shahsavari, E. (2017). Bioremediation of phenol-contaminated industrial wastewater using a bacterial consortium-from laboratory to field. *Water, Air & Soil Pollution*, 228, 89. DOI: 10.1007/s11270-017-3273-0.

[6] Khan, M.M., Adil, S.F., Al-Mayouf, A. (2015). Metal oxides as photocatalysts. *Journal of Saudi Chemical Society*, 19, 462–464. DOI: 10.1016/j.jscs.2015.04.003.

[7] Arora, A.K., Jaswal, V.S., Singh, K., Singh, R. (2016). Applications of metal/mixed metal oxides as photocatalyst: A review. *Oriental Journal of Chemistry*, 32, 2035–2042. DOI: 10.13005/ojc/320430.

[8] Yemmireddy, V.K., Hung, Y.-C. (2017). Using photocatalyst metal oxides as antimicrobial surface coatings to ensure food safety–Opportunities and challenges. *Comprehensive Reviews in Food Science and Food Safety*, 15, 617–631. DOI: 10.1111/1541-4337.12267.

[9] Pieczyńska, A., Malankowska, A., Bajorowicz, B., Gołąbiewska, A., Grabowska, E., Nadolna, J., Marchelek., M., Kobylański, M.P., Paszkiewicz-Gawron, M., Mazierski, P., Zaleska-Medynska, A., (2018). *Metal oxide-based photocatalysis Fundamentals and prospects for application*, 1st edition. Netherlands: Elsevier.

[10] Karthikeyan, C., Arunachalam, P., Ramachandran, K., Al-Mayouf, A.M., Karuppuchamy, S. (2020). Recent advances in semiconductor metal oxides with enhanced methods for solar photocatalytic applications. *Journal of Alloys and Compounds*, 828, 154281. DOI: 10.1016/j.jallcom.2020.154281.

[11] Yuliati, L., Siah, W.R., Roslan, N.A., Shamsuddin, M., Lintang, H.O. (2016). Modification of titanium dioxide nanoparticles with copper oxide co-catalyst for photocatalytic degradation of 2,4-dichlorophenoxyacetic acid. *Malaysian Journal of Analytical Science*, 20, 171–178. DOI: 10.17576/mjas-2016-2001-18.

[12] Yuliati, L., Hasan, N., Lintang, H.O. (2020). Copper oxide modification to improve the photocatalytic activity of titanium dioxide na-

noparticles: P25 versus P90. *IOP Conference Series: Materials Science and Engineering*, 902, 012020. DOI: 10.1088/1757-899X/902/1/012010.

[13] Yuliati, L., Roslan, N.A., Siah, W.R., Lintang, H.O. (2017). Cobalt oxide-modified titanium dioxide nanoparticles photocatalyst for degradation of 2,4-dichlorophenoxyacetic acid. *Indonesian Journal of Chemistry*, 17, 284–290. DOI: 10.22146/ijc.22624.

[14] Siah, W.R., Lintang, H.O., Shamsuddin, M., Yuliati, L. (2016). High photocatalytic activity of mixed anatase-rutile phases on commercial TiO_2 nanoparticles. *IOP Conference Series: Material Science and Engineering*, 107, 012005. DOI: 10.1088/1757-899X/107/1/012005.

[15] Nakata, K., Fujishima, A. (2012). TiO_2 photocatalysis: design and applications. *Journal of Photochemistry Photobiology C: Photochemistry Reviews*, 13, 169–189. DOI: 10.1016/j.jphotochemrev.2012.06.001.

[16] Kurniawan, Y.S., Anggraeni, K., Indrawati, R., Yuliati, L. (2020). Functionalization of titanium dioxide through dye-sensitizing method utilizing red amaranth extract for phenol photodegradation. *IOP Conference Series: Material Science and Engineering*, 902, 012029. DOI: 10.1088/1757-899X/902/1/012029

[17] Khang, K.C.L., Hatta, M.H.M., Lee, S.L., Yuliati, L. (2018). Photocatalytic removal of phenol over mesoporous ZnO/TiO_2 composites. *Jurnal Teknologi (Sciences and Engineering)*, 80, 153–160. DOI: 10.11113/jt.v80.11209.

[18] Siwinska-Stefanska, K., Kubiaka, A., Piasecki, A., Goscianska, J., Nowaczyk, G., Jurga, S., Jesionowski, T. (2018). TiO_2-ZnO binary oxide systems: comprehensive characterization and tests of photocatalytical activity. *Materials*, 11, 841. DOI: 10.3390/ma11050841.

[19] Yuliati, L., Salleh, A.M., Hatta, M.H.M., Lintang, H.O. (2018). Effect of preparation methods on the activity of titanium dioxide-carbon nitride composites for photocatalytic degradation of salicylic acid. *IOP Conference Series: Materials Science and Engineering*, 349, 012033. DOI: 10.1088/1757-899X/349/1/012033.

[20] Ayed, S., Belgacem, R.B., Zayani, J.O., Matoussi, A. (2016). Structural and optical properties of ZnO/TiO_2 composites. *Superlattices and Microstructures*, 91, 118–128. DOI: 10.1016/j.spmi.2016.01.004.

[21] Lu, P.J., Huang, S.C., Chen, Y.P., Chiueh, L.C., Shih, D.Y.C. (2015). Analysis of titanium dioxide and zinc oxide nanoparticles in cosmetics. *Journal of Food and Drug Analysis*, 23, 587–594. DOI: 10.1016/j.jfda.2015.02.009.

[22] Supriyanto, A., Kurniawan, D., Cari, C. (2020). Pengaruh perbandingan komposisi ZnO dan TiO_2 dalam Dye-Sensitized Solar Cell (DSSC) pada dye kangkong (Ipomea aquatica). *Prosiding Seminar Nasional Fisika dan Aplikasinya*, 1–9.

[23] Hussin, F., Lintang, H.O., Lee, S.L., Yuliati, L. (2018). Highly efficient zinc oxide-carbon nitride composite photocatalysts for degradation of phenol under UV and visible light irradiation. *Malaysian Journal of Fundamental and Applied Sciences*, Special issue on chromatography and other analytical techniques, 159–163. DOI: 10.11113/mjfas.v14n1-2.974.

[24] Abuzerr, S., Darwish, M., Mohammadi, A., Hosseini, S.S., Mahvi, A.H. (2018). Enhancement of reactive red 198 dye photocatalytic degradation using physical mixtures of ZnO-graphene nanocomposite and TiO_2 nanoparticles: an optimized study by response surface methodology. *Desalination and Water Treatment*, 135, 290–301. DOI: 10.5004/dwt.2018.232.59.

[25] Makuła, P., Pacia, M., Macyk, W. (2018). How to correctly determine the band gap energy of modified semiconductor photocatalysts based on UV-vis spectra. *The Journal of Physical Chemistry Letters*, 9, 6814–6817. DOI: 10.1021/acs.jpclett.8b02892.

[26] Kołodziejczak-Radzimska, A., Markiewicz, E., Jesionowski, T. (2012). Structural characterization of ZnO particles obtained by the emulsion precipitation method. *Journal of Nanomaterials*, 2012, 656353. DOI: 10.1155/2012/656353.

[27] Sethi, D., Sakthivel, R. (2017). ZnO/TiO_2 composites for photocatalytic inactivation of Escherichia coli. *Journal of Photochemistry and Photobiology B: Biology*, 168, 117–123. DOI: 10.1016/j.photobiol.2017.02.005.

[28] Devi, P.G., Velu, A.S. (2016). Synthesis, structural and optical properties of pure ZnO and Co doped ZnO nanoparticles prepared by the co-precipitation method. *Journal of Theory and Applied Physics*, 10, 233–240. DOI: 10.1007/s40094-016-0221-0.

[29] Babu, K.S., Reddy, A.R., Sujatha, C., Reddy, K.V., Mallika, A.N. (2013). Synthesis and optical characterization of porous ZnO. *Journal of Advanced Ceramics*, 2, 260–265. DOI: 10.1007/s40145-013-0069-6.

[30] Chen, X., Wu, Z., Liu, D., Gao, Z. (2017). Preparation of ZnO photocatalyst for the efficient and rapid photocatalytic degradation of azo dyes. *Nanoscale Research Letters*, 12, 143. DOI: 10.1186/s11671-017-1904-4.

[31] Pasikhani, J.V., Gilani, N., Pirbazari, A.E. (2018). Improvement the wastewater purification by TiO_2 nanotube arrays: the effect of etching-step on the photo-generated charge carriers and photocatalytic activity of anodic TiO_2 nanotubes. *Solid State Sciences*, 84, 57–74. DOI: 10.1016/j.solidstatesciences.2018.08.003.

[32] Lin, H.Y., Chou, Y.Y., Cheng, C.L., Chen, Y.F. 2007. Giant enhancement of band edge emission based on ZnO/TiO_2 nanocomposites. *Optics Express*, 15, 13832. DOI: 10.1364/OE.15.013832.

[33] Wang, R., Tan, H., Zhao, Z., Zhang, G., Song, L., Dong, W., Sun, Z. 2014. Stable ZnO@TiO_2 core/shell nanorod arrays with exposed high energy facets for self-cleaning coatings with anti-reflective properties. *Journal of Materials Chemistry*, 2, 7313–7318. DOI: 10.1039/C4TA00455H

[34] Lee, Y.E., Cao, T., Torruellas, C., Kozlowski, M.C. (2014). Selective oxidative homo- and cross-coupling of phenols with aerobic catalysts. *Journal of American Chemical Society*, 136, 6782–6785. DOI: 10.1021/ja500183z.

Selected and Revised Papers from 3rd International Conference on Chemistry, Chemical Process and Engineering 2020 (IC3PE 2020) (https://chemistry.uii.ac.id/ic3pe/) (Universitas Islam Indonesia (UII), Labuan Bajo, Nusa Tenggara Timur, Indonesia by 30th September – 1st October 2020) after Peer-reviewed by Scientific Committee of IC3PE 2020 and Peer-Reviewers of Bulletin of Chemical Reaction Engineering & Catalysis. Editors: Is Fatimah; I. Istadi